Inorg. Chem. **1992**, *31*, 21-26

Contribution from the Lehrstuhl für Anorganische Chemie I, Ruhr-Universität, D-4630 Bochum, Germany,
Institut für Physik, Medizinische Universität, D-2400 Lübeck, Germany,
and Anorganisch-Chemisches Institut der Universität, D-6900 Heidelberg, Germany

Coordination of 4,7-Bis(2-hydroxybenzyl)-1-oxa-4,7-diazacyclononane (LH_2) with Manganese(II) and -(III) and Zinc(II). Crystal Structure of $[(LH)_2Zn_2(\mu\text{-}OH)](PF_6)\cdot 0.5CH_3OH$

Claus Flassbeck,[1a] Karl Wieghardt,*,[1a] Eckhard Bill,[1b] Christian Butzlaff,[1b] Alfred X. Trautwein,[1b]
Bernhard Nuber,[1c] and Johannes Weiss[1c]

Received June 21, 1991

The pentadentate macrocyclic ligand 4,7-bis(2-hydroxybenzyl)-1-oxa-4,7-diazacyclononane (LH_2) has been prepared for the first time, and its coordination chemistry with manganese(II) and -(III) and zinc(II) has been investigated. From methanolic solutions of LH_2, $Mn(ClO_4)_2\cdot 6H_2O$, and $Zn(ClO_4)_2\cdot 6H_2O$, colorless crystals of $[(LH)_2Mn_2(\mu\text{-}OH)](ClO_4)$ and $[(LH)_2Zn_2(\mu\text{-}OH)](ClO_4)\cdot 7H_2O$ have been obtained, respectively. The crystal structure of $[(LH)_2Zn_2(\mu\text{-}OH)](PF_6)\cdot 0.5CH_3OH$ has been determined by X-ray crystallography. Crystal data: orthorhombic space group *Pncb*, $a = 12.254$ (5) Å, $b = 18.066$ (8) Å, $c = 19.605$ (9) Å, $Z = 4$. Two octahedrally coordinated zinc ions are connected by a μ-hydroxo bridge. The coordinated phenolate and phenolic groups of both LH^- ligands form two intramolecular O–H···O contacts. From temperature-dependent magnetic susceptibility measurements and EPR spectroscopy on $[(LH)_2Mn_2(\mu\text{-}OH)][B(C_6H_5)_4]$ an intramolecular antiferromagnetic exchange coupling constant, J, of $-2.65\ cm^{-1}$ has been determined ($H_{ex} = -2JS_1\cdot S_2$; $S_1 = S_2 = {}^5/_2$; $g = 2.0$). Deprotonation of the dinuclear Mn^{II} species by $N(C_2H_5)_3$ in CH_3CN affords monomeric five-coordinate LMn^{II}. $LMn^{III}X$ complexes (X = Cl, NCS, N_3) have also been prepared, as well as $[LZn(H_2O)ZnCl_2]$.

Introduction

Recently we[2] and others[3] have begun to explore the coordination chemistry of macrocyclic ligands containing a 1,4,7-triazacyclononane backbone and three N-bound pendent phenolate groups (Chart I). These hexadentate trianionic ligands have been shown to form extremely stable neutral complexes with trivalent first-row transition-metal ions and gallium(III).[3,4] Thus, for the iron(III) complex of the 3-hydroxy-6-methyl-2-pyridyl derivate (Chart I) a log β value of 49.98 and a pM value of 39.4 at pH 7.4 and 100% excess of ligand has been measured, which renders this ligand the strongest synthetic iron(III) chelator known to date.[4]

Here we report the synthesis of a pentadentate analogue derived from the nine-membered macrocycle 1-oxa-4,7-diazacyclononane.[5,6] 4,7-Bis(2-hydroxybenzyl)-1-oxa-4,7-diazacyclononane (LH_2) in its dianionic form (L) is pentadentate, leaving one coordination site available in a pseudooctahedral (or trigonal prismatic) complex. We have discovered that the ligand binds strongly to manganese(II) and -(III) and zinc(II). The most interesting feature of this study is the formation of μ-hydroxo-bridged dinuclear species $[(LH)_2M_2(\mu\text{-}OH)]^+$ (M = Mn(II), Zn(II)), where the coordinated pentadentate monoanionic ligands, LH^-, form two intramolecular O–H···O contacts between the phenolate and phenolic oxygen atoms of two adjacent ligands. From temperature-dependent susceptibility measurements and EPR spectroscopy, it is shown that the spins of the two d^5 high-spin manganese(II) ions are intramolecularly antiferromagnetically coupled.

Chart I

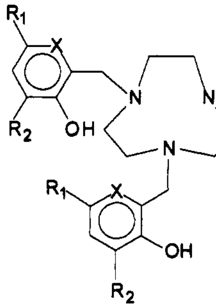

R_1	R_2	X	*Ref.*
H	H	CH	2
H	$C(CH_3)_3$	CH	2
CH_3	CH_3	CH	3
CH_3	H	N	4

Experimental Section

The macrocycle 1-oxa-4,7-diazacyclononane[5,6] and 2-(bromomethyl)phenyl acetate[7] were prepared according to literature procedures.

Synthesis of the Ligand. To a solution of 1-oxa-4,7-diazacyclononane (4.6 g; 35.4 mmol) in dry toluene (100 mL) was added finely powdered KOH (5.0 g; 88.5 mmol). A solution of 2-(bromomethyl)phenyl acetate (16.2 g; 70.8 mmol) in toluene (30 mL) was added dropwise to the above solution with stirring within 3 h at room temperature. The reaction mixture was stirred for 12 h at 20 °C after which time the solid residue (KBr; KOH) was removed by filtration and discarded. The solvent toluene was stripped off under reduced pressure. A light brown oil (14.4 g; 93%) of 4,7-bis(2-(acetyloxy)benzyl)-1-oxa-4,7-diazacyclononane was obtained to which was added a solution of methanol (100 mL) and sodium metal (2.0 g). The resulting clear solution was stirred at room temperature for 2 h. After addition of H_2O (150 mL) the solution was extracted three times with $CHCl_3$ (3 × 100 mL). The combined $CHCl_3$ phases were dried over $CaCl_2$. After rotary evaporation of the solvent the ligand was obtained as a light brown viscous oil, which was used for complex synthesis without further purification (yield: 9.2 g; 76%). ^1H NMR (80 MHz; $CDCl_3$; δ): 6.6–7.7 (m, 8 H), 3.85 (s, 4 H), 3.7 (t, 4 H), 3.0 (s, 4 H), 2.8 (t, 4 H).

Synthesis of Complexes. In the following we abbreviate the neutral ligand 4,7-bis(2-hydroxybenzyl)-1-oxa-4,7-diazacyclononane as LH_2 where both phenolate oxygen atoms are protonated. LH is the monoanion and L the dianion of this neutral ligand.

$[(LH)_2Mn_2(\mu\text{-}OH)](ClO_4)$. To a solution of the crude ligand LH_2 (0.34 g; 1 mmol) in methanol (10 mL) was added a methanolic solution (5 mL) of $Mn(ClO_4)_2\cdot 6H_2O$ (0.36 g; 1 mmol) at 60 °C. After the mixture was heated to reflux for 10 min, a colorless precipitate formed, which was filtered off and washed with methanol and diethyl ether and air-dried. When this reaction was carried out under an argon-blanketing atmosphere and cooled to 20 °C immediately after mixing of the two hot solutions, colorless, needle-shaped translucent crystals of the above complex formed within 24 h (yield: 0.45 g; 62%). Anal. Calcd for $C_{40}H_{51}N_4O_7Mn_2ClO_4$: C, 52.9; H, 5.6; N, 6.2; ClO_4, 11.0. Found: C, 53.1; H, 5.7; N, 6.0; ClO_4, 10.9.

The tetraphenylborate salt of the above complex was prepared analogously. One minute after the two above hot solutions were mixed, a

---

(1) (a) Ruhr-Universität Bochum. (b) Medizinische Universität Lübeck. (c) Universität Heidelberg.

(2) Auerbach, U.; Eckert, U.; Wieghardt, K.; Nuber, B.; Weiss, J. *Inorg. Chem.* **1990**, *29*, 938.

(3) Moore, D. A.; Fanwick, P. E.; Welch, M. J. *Inorg. Chem.* **1989**, *28*, 1504.

(4) Martell, A. E.; Motekaitis, R. J.; Welch, M. J. *J. Chem. Soc., Chem. Commun.* **1990**, 1748.

(5) Reinen, D.; Ozarowski, A.; Jacobi, B.; Pebler, J.; Stratemeyer, H.; Wieghardt, K.; Tolksdorf, I. *Inorg. Chem.* **1987**, *26*, 4010.

(6) Hancock, R. D.; Bharan, R.; Wade, P. W.; Boyens, J. C. A.; Dobson, S. M. *Inorg. Chem.* **1989**, *28*, 187.

(7) Karlin, K. D.; Cohen, B. I.; Hayes, J. C.; Farooq, A.; Zubieta, J. *Inorg. Chem.* **1987**, *26*, 147.

0020-1669/92/1331-0021$03.00/0

Table I. Crystallographic Data for $[(LH)_2Zn_2(\mu\text{-}OH)](PF_6)\cdot 0.5CH_3OH$

formula	$C_{40}H_{31}N_4O_7Zn_2PF_6\cdot$ $0.5CH_4O$	Z	4
		T, °C	22
fw	970.8	λ(Mo Kα), Å	0.71073
space group	D_{2h}^4, *Pncb* (No. 50)	ρ_{calcd}, g·cm^{-3}	1.48
a, Å	12.254 (5)	μ, cm^{-1}	12.4
b, Å	18.066 (8)	transm coeff	0.613–0.990
c, Å	19.605 (9)	$R(F_o)^a$	0.059
V, Å^3	4340.17	$R_w(F_o)^b$	0.050

^{a} $R(F_o) = \sum|\Delta F|/\sum|\Delta F_o|$. ^{b} $R_w(F_o) = [\sum w\Delta F^2/\sum|\Delta F_o|^2]^{1/2}$; $w = 1/\sigma^2(F)$.

solution of $Na[BPh_4]$ (0.68 g; 2 mmol) in methanol (5 mL) was added, which initiated the precipitation of white microcrystals of $[(LH)_2Mn_2(\mu\text{-}OH)](BPh_4)$. These were immediately filtered off, washed with CH_3OH and ether, and air-dried (yield: 0.45 g; 62%). Anal. Calcd for $C_{40}H_{51}N_4O_7Mn_2B(C_6H_5)_4$: C, 68.0; H, 6.3; N, 5.0. Found: C, 68.0; H, 6.3; N, 4.8.

LMn. To a solution of $[(LH)_2Mn_2(\mu\text{-}OH)](ClO_4)$ (0.18 g; 0.20 mmol) in acetonitrile (5 mL) was added triethylamine (0.05 g; 0.5 mmol), which initiated the immediate precipitation of a white solid (yield: 0.12 g; 75%). Anal. Calcd for $C_{20}H_{24}N_2O_3Mn$: C, 60.7; H, 6.1; N, 7.1. Found: C, 60.5; H, 6.5; N, 7.1.

$LMn^{III}X$ (X = Cl, NCS, N_3). To a refluxing reaction mixture of manganese(III) acetate[8] (0.32 g) in methanol (10 mL) was added a solution of the ligand (0.17 g; 0.5 mmol) in CH_3OH (5 mL). After 15 min of heating to reflux, a clear deep brown solution was obtained to which LiCl (0.04 g; 1.0 mmol), NaSCN (0.08 g; 1.0 mmol), and NaN_3 (0.065 g; 1.0 mmol) were added, respectively. This solution was heated to reflux for another 10 min. Upon cooling of the solution to 20 °C, green precipitates of the desired complexes formed, which were collected by filtration, washed with methanol and ether, and air-dried (yield: ≈ 80%). Anal. Calcd for $C_{20}H_{24}N_2O_3MnCl$: C, 55.8; H, 5.6; N, 6.5. Found: C, 56.0; H, 5.7; N, 6.4. Calcd for $C_{21}H_{24}N_3O_3MnS\cdot H_2O$: C, 53.4; H, 5.5; N, 8.9. Found: C, 53.6; H, 5.2; N, 8.8. IR (KBr, cm$^{-)}$: ν(NCS) 2049. Anal. Calcd for $C_{20}H_{24}N_5O_3Mn$: C, 54.9; H, 5.5; N, 16.0. Found: C, 54.7; H, 5.7; N, 16.0. IR (KBr, cm$^{-)}$: $\nu(N_3)$ 2054. UV–vis spectrum for LMnCl (CH_3CN) [λ_{max}, nm (ϵ, L mol^{-1} cm^{-1})]: 252 (1.7 × 10^4), 300 sh, 365 (4.7 × 10^3), 452 (1.7 × 10^3), 580 (430), 765 (365).

$[(LH)_2Zn_2(\mu\text{-}OH)](ClO_4)\cdot 7H_2O$. Heating to reflux for 15 min of a solution of the crude ligand (0.34 g; 1.0 mmol) in methanol (10 mL), to which a CH_3OH solution (5 mL) of $Zn(ClO_4)_2\cdot 6H_2O$ (0.37 g; 1.0 mmol) was added, resulted in the formation of a white solid, which was collected by filtration, washed with methanol and ether, and air-dried (yield: 0.39 g; 74%). Anal. Calcd for $C_{40}H_{51}N_4O_7Zn_2ClO_4\cdot 7H_2O$: C, 45.5; H, 6.2; N, 5.3. Found: C, 45.5; H, 5.9; N, 5.2.

The hexafluorophosphate hemimethanol salt was obtained when $NaPF_6$ (0.32 g; 2 mmol) dissolved in methanol (5 mL) was added to the above reaction mixture immediately after mixing of the two CH_3OH solutions. Recrystallization from an acetonitrile/methanol mixture (90:10) produced colorless, translucent single crystals which were suitable for an X-ray structure determination.

$[LZn(H_2O)ZnCl_2]\cdot 0.5CH_3CN$. To a solution of the crude ligand (0.34 g; 1.0 mmol) in methanol (10 mL) was added $ZnCl_2$ (0.28 g; 2 mmol) dissolved in methanol (5 mL). After the solution was heated to reflux for 10 min, a colorless precipitate formed upon cooling to 20 °C. The precipitate was recrystallized from an acetonitrile/methanol mixture (1:1) (yield: 0.45 g; 78%). Anal. Calcd for $C_{20}H_{26}N_2O_4Zn_2Cl_2\cdot 0.5CH_3CN$: C, 43.4; H, 4.7; N, 6.0; Cl, 12.2. Found: C, 43.6; H, 5.0; N, 5.9; Cl, 12.0.

X-ray Structure Determination. Intensities and lattice parameters of a colorless crystal of $[(LH)_2Zn_2(\mu\text{-}OH)](PF_6)\cdot 0.5CH_3OH$ were measured on a Syntex R3 diffractometer at ambient temperature. Crystal parameters and details of the data collection are given in Table I (for full details see Table S1 in the supplementary material). Empirical absorption corrections (ψ scans of seven reflections with $8.3 < 2\theta < 43.5°$) were carried out.[9] The structure was solved with conventional Patterson and difference Fourier methods. The function minimized during full-matrix least-squares refinement was $\sum w(|F_o| - |F_c|)^2$, where $w = 1/\sigma^2(F)$. Neutral-atom scattering factors and anomalous dispersion corrections were taken from ref 10. The positions of H atoms bound to carbon atoms were calculated (C–H = 0.96 Å) and included in the refinement cycle with a common isotropic parameter ($U_{ISO} = 0.080$ Å^2). Both phenoxy protons and also the proton of the hydroxo bridge have been located in the final difference Fourier map but were not refined. They were included in the final refinement cycle.

Scheme I

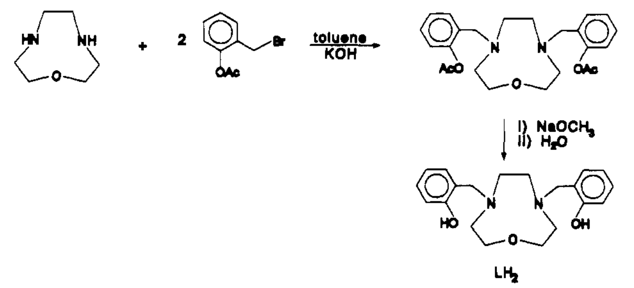

Electron Paramagnetic Resonance and Magnetic Susceptibility Measurements. EPR spectra were recorded on a Bruker ER 200D X-band spectrometer, equipped with a standard TE 102 resonator (ER 4102, Bruker) and a helium-flow cryostat (ESR 910, Oxford Instruments). The sample was in a standard 4-mm quartz tube. The temperature control was calibrated using the Curie–Weiss behavior of a Cu(II)–EDTA standard.[11] From measurements with a carbon–glass resistor in a test sample the temperature gradient was estimated to be less than 0.3 K over the sample volume. Microwave frequency and magnetic field were measured with a frequency counter and an NMR field meter, respectively.

Temperature-dependent magnetic susceptibilities were measured with a SQUID magnetometer (MPMS, Quantum Design). The sample material was contained in a 4-mm quartz tube. Data were evaluated using the standard software of the instrument and corrected for the diamagnetic response of the holder.

Results and Discussion

The ligand LH_2 was synthesized in a straightforward reaction of 1-oxa-4,7-diazacyclononane with 2 equiv of 2-(bromomethyl)phenyl acetate in toluene over KOH yielding 4,7-bis(2-(acetyloxy)benzyl)-1-oxa-4,7-diazacyclononane, which was hydrolyzed with $CH_3OH/NaOCH_3$ and water to give the uncoordinated ligand 4,7-bis(2-hydroxybenzyl)-1-oxa-4,7-diazacyclononane (LH_2) in good yields (Scheme I).

The reaction of methanolic solutions of LH_2 with $Mn(ClO_4)_2\cdot 6H_2O$ and $Zn(ClO_4)_2\cdot 6H_2O$ affords colorless precipitates, respectively, which analyzed as $[(LH)_2M_2(\mu\text{-}OH)](ClO_4)\cdot nH_2O$ ($M = Mn^{II}$, $n = 0$; $M = Zn^{II}$, $n = 7$). Colorless, translucent crystals of $[(LH)_2Mn_2(\mu\text{-}OH)]BPh_4$ and $[(LH)_2Zn_2(\mu\text{-}OH)]$-$[(PF_6)\cdot 0.5CH_3OH$ have also been prepared by metathesis reactions. From the latter material the crystal structure has been determined (see below). On the basis of these results we propose that the manganese(II) complex has the same structure:

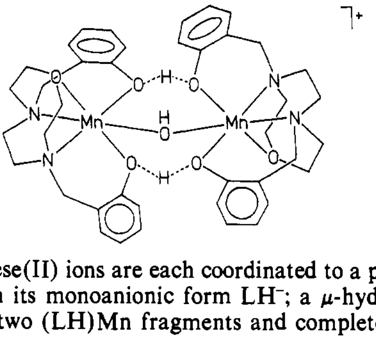

Two manganese(II) ions are each coordinated to a pentadentate macrocycle in its monoanionic form LH^-; a μ-hydroxo bridge connects the two (LH)Mn fragments and completes the pseudooctahedral environment at each Mn(II) ion. The phenolate and phenolic groups of each ligand form an intramolecular O–H···O contact to the other ligand. These cooperative hydrogen bonds

---

(8) The compound often referred to as "manganese(III) acetate" is in fact $[Mn_3(\mu\text{-}O)(\mu\text{-}CH_3CO_2)_6(H_2O)_3]CH_3CO_2$.

(9) Computations were carried out on an Microvax II computer by using the SHELXTL PLUS program package (Sheldrick, G. M. Universität Göttingen, revision 3.4, 1988).

(10) *International Tables for X-ray Crystallography*; Kynoch: Birmingham, England, 1974; Vol. IV, pp 99, 149.

(11) Slappendel, S.; Veldink, G. A.; Vliegenhardt, J. F. G.; Aasa, R.; Malmström, B. *Biochim. Biophys. Acta* **1980**, *624*, 30.

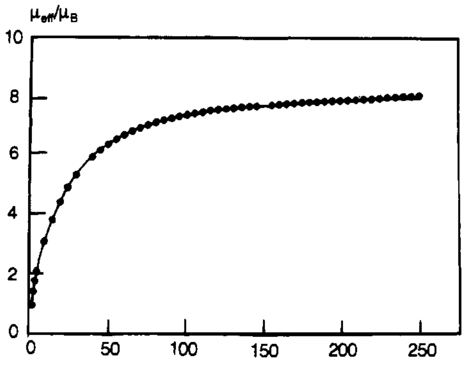

Figure 1. Temperature dependence of the magnetic moment of $[(LH)_2Mn_2(\mu\text{-}OH)][BPh_4]$ (μ_{eff}/dinuclear unit) measured in an applied field of 1 T. Circles represent experimental data, and the solid line is a least-squares fit to eq 1.

give rise to a very broad absorption in the infrared spectrum between 1600 and 400 cm^{-1}.[12] $[(LH)_2Mn_2(\mu\text{-}OH)](ClO_4)$ is soluble in acetonitrile and air-stable both in solution and in the solid state. Addition of 2 equiv of triethylamine initiates the immediate precipitation of colorless solid LMn^{II}, which is again not sensitive to oxygen. We propose a five-coordinate neutral monomeric species, since magnetic susceptibility measurements on a solid sample indicate the absence of any appreciable intra- or intermolecular spin-exchange coupling (see below).

The reaction of the macrocyclic ligand dissolved in methanol with 2 equiv of $ZnCl_2$ at elevated temperatures affords colorless crystals of $[LZn(OH_2)ZnCl_2]$, the structure of which has been determined by X-ray crystallography.

Pseudooctahedral, deep green complexes of manganese(III), $[LMn^{III}X]$, containing a coordinated pentadentate ligand dianion and a unidentate anionic sixth ligand such as chloride, thiocyanate, or azide have been prepared from refluxing methanolic solutions of "manganese(III) acetate",[8] the ligand LH_2, and LiCl, NaSCN, and NaN_3, respectively. For these pseudooctahedral LMX complexes there are, in principle, two geometric isomers, namely A and B.

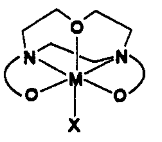

A

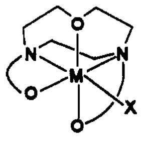

B

We have not been able to grow suitable single crystals for an X-ray structure determination of either of the LMnX species and, therefore, cannot definitively decide which of these structures prevails.

Magnetism and EPR Spectroscopy. The magnetic susceptibility of a powdered sample of LMn^{II} has been measured in the temperature range 89–298 K by using the Faraday method. A temperature-independent magnetic moment of 5.7 μ_B is in agreement with the spin-only value expected for a mononuclear manganese(II) complex with d^5 high-spin electron configuration. Similar measurements have been carried out on powdered samples of $LMn^{III}X$ complexes where temperature-independent magnetic moments of 4.7 μ_B for X = Cl, 4.95 μ_B for X = NCS, and 5.0 μ_B for $X = N_3^-$ have been determined, which are indicative of a d^4 high-spin electron configuration.

For $[(LH)_2Mn_2(\mu\text{-}OH)][BPh_4]$ as well as its perchlorate analogue the magnetic moments were found to follow a temperature dependence. With decreasing temperature the magnetic moment decreases, which is typical for an intramolecularly antiferromagnetically coupled dinuclear species. Figure 1 shows the magnetic moment per dinuclear unit of the tetraphenylborate salt as a function of temperature in the range 4.2–250 K. The solid line represents a spin Hamiltonian simulation by using eq 1, where $J = -2.65\ cm^{-1}$, $g_1 = g_2 = 2.0$ (fixed), $S_1 = S_2 = {}^5/_2$, and $D_1 = D_2 = 0.7\ cm^{-1}$.

Chart II

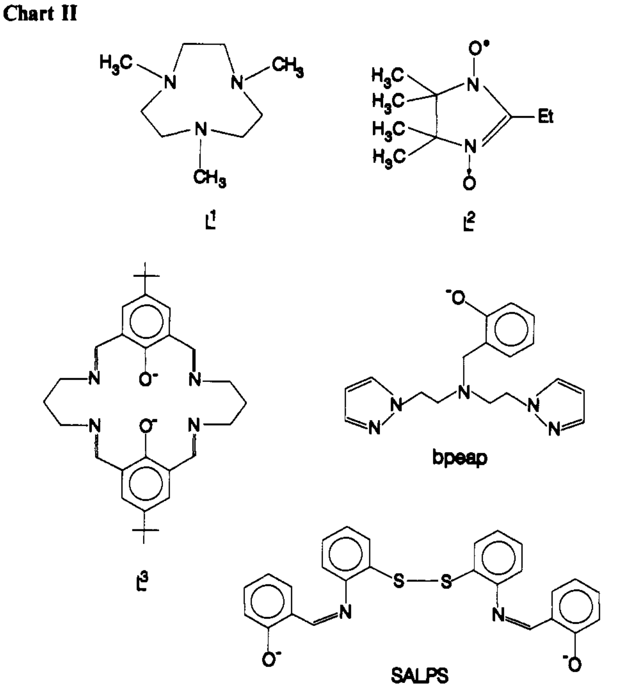

Table II. Spin-Exchange Coupling in Dinuclear Manganese(II) Complexes[a]

	J, cm^{-1} [b]	g	ref
$[L^1_2Mn_2(\mu\text{-}OH)(\mu\text{-}OAc)_2](ClO_4)$	−9	2.00	13
$[L^2_2Mn_2(OR)_2(OH_2)_2(\mu\text{-}OH_2)(\mu\text{-}OR)_2]$[c]	−1.65	2.02	14
$[L^3_2Mn_2Cl_2]\cdot 0.5CH_3OH$	0.24	1.97	15a
$[Mn(bpeap)(THF)]_2(ClO_4)_2$	<−0.18	?	15b
$[Mn(SALPS)]_2$	−1.88	2	15c

[a] The structures of the ligands are shown in Chart II. [b] $H = -2J(S_1S_2)$; $S_1 = S_2 = {}^5/_2$. [c] $R = F_5C_2CO$.

$$H = D_1(S_z^2 - {}^{35}/_{12}) + \mu_B\vec{B}g_1\vec{S}_1 + D_2(S_z^2 - {}^{35}/_{12}) + \mu_B\vec{B}g_2\vec{S}_2 - 2J(\vec{S}_1\vec{S}_2) \quad (1)$$

It is noted that the fit does not depend strongly on the numerical value of the zero-field splitting parameter, D. Therefore, the value should not be taken too seriously. The perchlorate salt, where the dinuclear cations are more closely packed, gave very similar results, which indicates that intermolecular spin-exchange coupling in the solid state is negligible in both salts.

Table II summarizes pertinent magnetic data of some structurally characterized μ-hydroxo-,[13] μ-aqua-,[14] and μ-phenoxo[15]-bridged dinuclear manganese(II) complexes. The μ-aqua and μ-phenoxo bridges provide the weakest spin exchange coupling pathways, whereas μ-hydroxo-bridged species are more strongly antiferromagnetically coupled. This is most probably due to the fact that the Mn–O distance decreases in the order μ-aqua > μ-phenoxo > μ-hydroxo.

---

(12) (a) Hadzi, D. *Pure Appl. Chem.* **1965**, *11*, 435. (b) Bratus, S.; Ratajczak, K. *J. Chem. Phys.* **1982**, *76*, 77.

(13) (a) Wieghardt, K.; Bossek, U.; Nuber, B.; Weiss, J.; Bonvoisin, J.; Corbella, M.; Vitols, S. E.; Girerd, J. J. *J. Am. Chem. Soc.* **1988**, *110*, 7398. (b) Bossek, U.; Wieghardt, K.; Nuber, B.; Weiss, J. *Inorg. Chim. Acta* **1989**, *165*, 123.

(14) Caneschi, A.; Ferraro, F.; Gatteschi, D.; Chiaro Melandui, M.; Rey, P.; Sessoli, R. *Angew. Chem., Int. Ed. Engl.* **1989**, *28*, 1365.

(15) (a) Chang, H. R.; Larsen, S. K.; Boyd, P. D. W.; Pierpont, C. G.; Hendrickson, D. N. *J. Am. Chem. Soc.* **1988**, *110*, 4565. (b) Hodgson, D. J.; Schwartz, B. J.; Sorrell, T. N. *Inorg. Chem.* **1989**, *28*, 2226. (c) Kessissoglou, D. P.; Butler, W. M.; Pecoraro, V. L. *Inorg. Chem.* **1987**, *26*, 495.

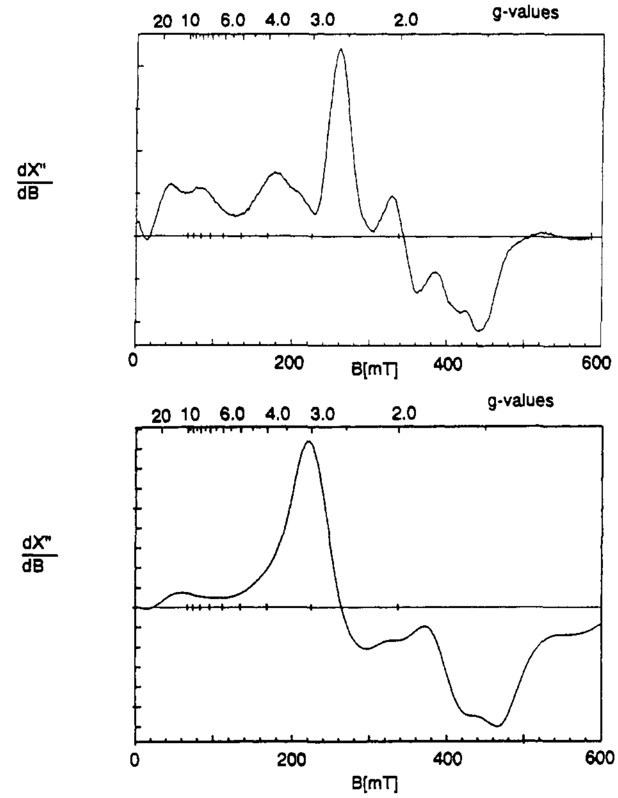

Figure 2. X-Band EPR spectra of solid $[(LH)_2Mn^{II}_2(\mu\text{-}OH)][BPh_4]$ (top) and LMn^{II} (bottom) at 10 K (microwave frequency 9.435 GHz).

Figure 2 shows solid-state X-band EPR spectra of the dinuclear complex $[(LH)_2Mn_2(\mu\text{-}OH)]BPh_4$ (top) and of the mononuclear species LMn (bottom) at 10 K. Complicated, unsymmetrical multiple-signal spectra without apparent hyperfine splitting are observed in both cases. Similar spectra have been observed for monomeric as well as for dimeric Mn(II) Schiff base complexes.[15c] The structure of the monomer spectrum indicates the Mn(II) ion to be in the high-spin state ($S = {}^5/_2$) and to experience a ligand field with distorted symmetry ($E/D \neq 0$) and, most importantly, with weak zero-field splitting $D < h\nu$ ($h\nu = 0.3$ cm^{-1} for $\nu = 9.43$ GHz). Low-spin Mn(II) would exhibit a spectrum with three resolved lines at g factors close to 2. On the other hand, a high-spin complex with strong zero-field splitting, $D \gg h\nu$, the electronic sublevels of the spin sextet would be grouped in three Kramers doublets with distinct effective g factors.[16] In the limiting cases of axial and rhombic symmetry, spectra with strong resonances at $g = 6$ and 2 or with an isotropic line at $g = 4.3$, respectively, are predicted. However, the spreading of resonances in the monomer spectra in the whole range of the applied field reveals multiple transitions within the spin sextet, accessible to the 9.43-GHz microwave radiation. The powder distribution of molecular orientations relative to the applied field leads to a further variation of resonances.

The interpretation of the dinuclear Mn(II) spectra is even more intriguing than those of the mononuclear species, which is due to the large number of possible $\Delta m = 1$ transitions in the six manifolds of total spin S = 0–5 in the coupled system of spins $S_1 = S_2 = {}^5/_2$. Powder integration and probable "$\Delta m \neq 1$" transitions will further complicate the situation. Therefore, we refrained from a detailed analysis of these spectra. Nevertheless, we could evaluate an important spectral feature. In contrast to the monomeric case, the relative intensities of "lines" in the spectra of the dinuclear species are significantly temperature dependent (Figure 3). In particular, the relative amplitudes of the signal at $g \approx 2.65$ appear to grow with increasing temperature to reach

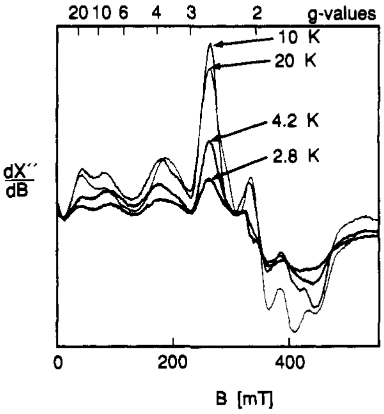

Figure 3. Temperature dependence of the X-band EPR spectrum in the range 2.7–20 K of solid $[(LH)_2Mn_2(\mu\text{-}OH)]BPh_4$.

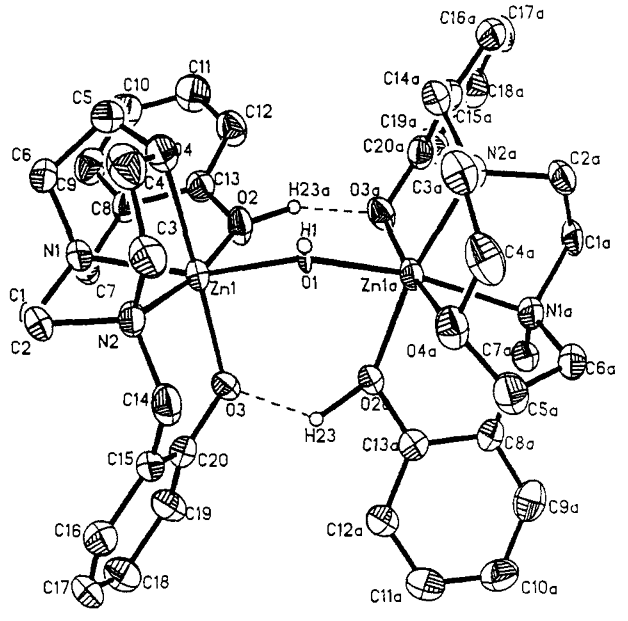

Figure 4. Perspective view of the cation in crystals of $[(LH)_2Zn_2(\mu\text{-}OH)]PF_6{\cdot}0.5CH_3OH$ and atom-labeling scheme.

a maximum at about 15 K and then decrease again with further warming up. Such a behavior is typical for resonances in excited states, which are populated with increasing temperature. In first order, the Boltzmann population of the multiplet in which the resonance occurs is proportional to the EPR intensity I times temperature T:

$$IT \approx \exp(-E(i)/kT)/Z \qquad (2)$$

Here $E(i)$ is the energy of the resonating multiplet i and Z is the partition function of the system. We adopted an antiferromagnetic exchange interaction and energy separations of $2J$, $6J$, $12J$, and $30J$ between the spin manifolds S = 0–5, in accordance with eq 1, with negligible zero-field splittings of the local $S = {}^5/_2$ spin states. Substituting the corresponding partition function $Z = 1 + 3\exp(-2J/kT) + 5\exp(-6J/kT) + 7\exp(-12J/kT) + 9\exp(-20J/kT) + 11\exp(-30J/kT)$ and the energy $E(1) = 2J$ for the first excited $S = 1$ spin multiplet in eq 2 and fitting the relative amplitudes of the signal at $g \approx 2.65$ (Figure 3) yielded $J = -8$ cm^{-1} for the exchange-coupling constant, which is much larger than the value obtained from magnetic susceptibility data. However, with the assumption that the corresponding resonance originates from transitions in the second excited $S = 2$ spin multiplet, which is at energy $E(2) = 6J$, we obtain $J = -2.67$ cm^{-1}. This value is in striking agreement with the value derived from susceptibility measurements. Thus, this EPR signal is assigned

---

[16] Trautwein, A. X.; Bill, E.; Bominaar, E.; Winkler, M. *Structure and Bonding*; Springer Verlag: Berlin, 1991; Vol. 78, in press.

Table III. Atom Coordinates ($\times 10^4$) and Temperature Factors ($Å^2 \times 10^3$) for $[(LH)_2Zn_2(\mu\text{-}OH)](PF_6)\cdot 0.5CH_3OH$

atom	*x*	*y*	*z*	*U*(eq)[a]
Zn1	8624 (1)	60 (1)	2783 (1)	35 (1)
O1	10000	−389 (2)	2500	21 (1)
O2	9486 (3)	827 (2)	3367 (2)	47 (1)
O3	8569 (3)	732 (2)	1951 (2)	41 (1)
O4	8602 (3)	−869 (2)	3592 (2)	50 (1)
N1	7190 (3)	328 (3)	3369 (2)	38 (2)
N2	7573 (3)	−727 (2)	2328 (2)	36 (2)
C1	6311 (4)	178 (3)	2869 (3)	43 (2)
C2	6426 (4)	−593 (3)	2563 (3)	42 (2)
C3	7981 (5)	−1461 (3)	2548 (3)	50 (2)
C4	8071 (5)	−1511 (3)	3316 (4)	62 (3)
C5	8096 (5)	−553 (3)	4184 (3)	53 (2)
C6	7054 (4)	−135 (3)	3993 (3)	47 (2)
C7	7232 (4)	1134 (3)	3522 (3)	43 (2)
C8	8053 (5)	1315 (3)	4063 (3)	41 (2)
C9	7755 (5)	1644 (3)	4675 (3)	54 (2)
C10	8496 (6)	1805 (4)	5188 (3)	58 (3)
C11	9574 (6)	1619 (4)	5084 (3)	61 (3)
C12	9904 (5)	1301 (3)	4488 (3)	52 (2)
C13	9167 (5)	1152 (3)	3965 (3)	42 (2)
C14	7662 (5)	−667 (3)	1571 (3)	47 (2)
C15	7244 (4)	62 (4)	1308 (3)	42 (2)
C16	6358 (5)	62 (4)	863 (3)	52 (2)
C17	5968 (5)	723 (5)	610 (3)	65 (3)
C18	6448 (5)	1379 (4)	793 (3)	63 (3)
C19	7335 (5)	1381 (4)	1246 (3)	54 (2)
C20	7732 (5)	720 (3)	1505 (3)	42 (2)
P1	5000	7500	1085 (2)	51 (1)
F11	5165 (5)	6660 (3)	1093 (5)	168 (4)
F12	4116 (12)	7410 (13)	1640 (10)	148 (9)
F13	5788 (24)	7566 (19)	582 (11)	263 (19)
F14	5000	7500	271 (18)	233 (26)
F15	3781 (12)	7402 (10)	1009 (15)	179 (16)
F16	5000	7500	1793 (16)	302 (30)
O21	9410 (16)	2500	2500	122 (10)
C22	8407 (21)	2500	2500	85 (10)

[a] Equivalent isotropic *U* defined as one-third of the trace of the orthogonalized $\mathbf{U}_{ij}$ tensor.

Table IV. Selected Bond Distances (Å) and Angles (deg) for $[(LH)_2Zn_2(\mu\text{-}OH)](PF_6)\cdot 0.5CH_3OH$

Zn1–N1	2.154 (4)	Zn1–N2	2.115 (4)
Zn1–O1	1.915 (2)	Zn1–O2	2.086 (4)
Zn1–O3	2.033 (4)	Zn1–O4	2.310 (4)
O2–H23a	1.196	O3–H23	1.715
O1–H1	0.576	O3–O2a	2.469
O1–Zn1–O2	89.7 (1)	O2–Zn1–N2	170.6 (2)
O1–Zn1–O3	92.8 (1)	O3–Zn1–O4	169.7 (1)
O1–Zn1–O4	84.4 (1)	O3–Zn1–N1	105.5 (2)
O1–Zn1–N1	161.7 (1)	O3–Zn1–N2	92.5 (2)
O1–Zn1–N2	97.3 (1)	O4–Zn1–N1	77.7 (2)
O2–Zn1–O3	93.5 (1)	O4–Zn1–N2	78.1 (2)
O2–Zn1–O4	96.4 (1)	N1–Zn1–N2	83.1 (2)
O2–Zn1–N1	88.3 (2)	O3–H23–O2a	114.8
Zn1–O3–H23	127.6	Zn1–O1–Zn1a	130.8 (2)

to a transition within the $S = 2$ state.

Crystal Structures. Crystals of $[(LH)_2Zn_2(\mu\text{-}OH)](PF_6)\cdot 0.5CH_3OH$ consist of dinuclear monocations $[(LH)_2Zn_2(\mu\text{-}OH)]^+$, hexafluorophosphate anions, and methanol crystal solvent molecules. Table III gives the atom coordinates, and Table IV summarizes important bond distances and angles; Figure 4 shows a perspective view of the monocation. Each of the two zinc ions is in an octahedral environment composed of a pentadentate macrocyclic ligand and a bridging hydroxo group which connects the two zinc ions. The dication possesses crystallographic site symmetry C_2. The macrocyclic ligand is coordinated in its monoanionic form LH^-. One of each phenolate oxygen atom per ligand is protonated. This proton is also hydrogen bonded to the unprotonated phenolate oxygen located at the second ligand. Thus two intramolecular O–H···O contacts are formed (O···O = 2.469 Å). Both these protons and, in addition, the proton of the hydroxo bridge have been located in the final difference Fourier map. The O–H···O bond is unsymmetrical: O2–H23a = 1.20 Å and O3···H23a = 1.72 Å.

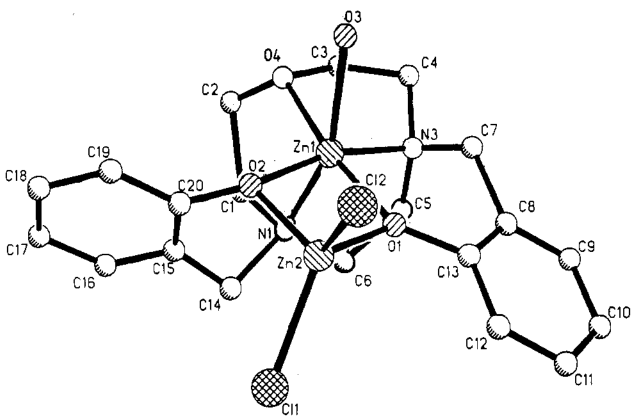

Figure 5. Ball-and-stick representation of the atom connectivity of the neutral molecule in crystals of $[LZn(OH_2)ZnCl_2]\cdot 0.5CH_3CN$.

As pointed out above, there are, in principle, two geometrical isomers, A and B, depending on the mode of coordination of the pentadentate macrocycle. In the dinuclear monocation both coordinated macrocyclic ligands LH^- adopt the geometry of isomer B where the coordinated ether oxygen atom O4 is in trans position with respect to a coordinated phenolate oxygen. Interestingly, in the trinuclear copper complex $[L_2Cu_3(H_2O)](ClO_4)\cdot 2H_2O$,[17] the two Cu(II) ions each containing a coordinated dianion L^{2-} adopt structure A with the sixth coordination site X unoccupied (square-based pyramidal coordination with the ether oxygen in the axial position).

The Zn–N and Zn–O phenoxo distances are quite similar to those in $[L'Zn(OH_2)](ClO_4)$,[18] where L′ represents the tetradentate macrocycle 2-(2-hydroxybenzyl)-1,5,9-triazacyclododecane. Here the Zn(II) ion is in a trigonal-bipyramidal environment (N_3O_2 donor set).

Crystals of $[LZn(H_2O)ZnCl_2]\cdot 0.5CH_3CN$ are poorly crystalline and are not really suitable for a high-quality X-ray structure analysis. Since this structural type has been proposed previously without characterization by X-ray diffraction methods for $[(tsb)M^1M^2Cl_2]$ complexes,[19] where tsb represents a tetradentate Schiff base ligand and $M^1 = M^2$ are Cu(II) or Zn(II), we decided to undertake a structure determination in order to establish the atom connectivity. Crystals of $[LZn(H_2O)ZnCl_2]\cdot 0.5CH_3CN$ crystallize in the hexagonal space group C_3^2 ($P3_1$ (No. 144)) with unit cell dimensions $a = 16.991$ (8) Å and $c = 19.98$ (1) Å.

The bond distances and angles are chemically reasonable although the estimated standard deviations are quite large ($\sigma \approx 0.03$ Å). Figure 5 shows a perspective view of the dinuclear neutral molecule $[L_2Zn_2(OH_2)ZnCl_2]$. From these data we conclude that the atom connectivity and, hence, the overall geometry of the molecule has been correctly established.

One of the zinc ions is octahedrally coordinated to a pentadentate macrocyclic ligand dianion in the same fashion as in the previous structure; the sixth coordination site is occupied by a water molecule. The second zinc ion is tetrahedrally coordinated to two chloride ions and to two bridging phenolate oxygen atoms. The Zn···Zn distance is at 3.08 Å.

Acknowledgment. We thank the Deutsche Forschungsgemeinschaft and the Fonds der Chemischen Industrie for financial support.

Registry No. LH_2, 137203-56-6; $[(LH)_2Mn_2(\mu\text{-}OH)](ClO_4)$, 137203-58-8; $[(LH)_2Mn_2(\mu\text{-}OH)](BPh_4)$, 137328-87-1; LMn, 137203-

---

(17) Flassbeck, C.; Wieghardt, K.; Nuber, B.; Weiss, J. *Z. Naturforsch.*, in press.

(18) Kimura, E.; Koike, T.; Toriumi, K. *Inorg. Chem.* **1988**, *27*, 3687.

(19) (a) Gruber, S. J.; Harris, C. M.; Sinn, E. *J. Inorg. Nucl. Chem.* **1968**, *30*, 1805. (b) Gruber, S. J.; Harris, C. M.; Sinn, E. *Inorg. Chem.* **1968**, *7*, 268.

61-3; $\mathrm{LMn^{III}Cl}$, 137203-62-4; $\mathrm{LMn^{III}NCS}$, 137203-63-5; $\mathrm{LMn^{III}N_3}$, 137203-64-6; $\mathrm{[(LH)_2Zn_2(\mu\text{-}OH)](ClO_4)}$, 137203-60-2; $\mathrm{[(LH)_2Zn_2(\mu\text{-}OH)](PF_6)\cdot 0.5CH_3OH}$, 137331-20-5; $\mathrm{[LZn(H_2O)ZnCl_2]\cdot 0.5CH_3CN}$, 137203-66-8; 1-oxa-4,7-diazacyclononane, 80289-59-4; 2-(bromomethyl)phenyl acetate, 704-65-4; 4,7-bis(2-(acetyloxy)benzyl)-1-oxa-4,7-diazacyclononane, 137203-55-5.

Supplementary Material Available: Listings of crystallographic data, calculated positions and thermal parameters of hydrogen atoms, bond lengths and bond angles, and anisotropic thermal parameters for $\mathrm{[(LH)_2Zn_2(\mu\text{-}OH)](PF_6)\cdot 0.5CH_3OH}$ (6 pages); a table of structure factors (18 pages). Ordering information is given on any current masthead page.

Contribution from the Department of Chemistry, Waseda University, Tokyo 169, Japan,
Department of Chemistry, Toho University, Funabashi, Chiba 274, Japan,
and Instrumental Analysis Center of Chemistry, Faculty of Science, Tohoku University, Aramaki Aoba, Aoba-ku, Sendai 980, Japan

Syntheses, Structures, and Reactivities of the Sulfur-Bridged Trinuclear Complexes $\mathrm{[(L)Ru(CO)(PPh_3)]_2(\mu\text{-}MS_4)}$ (L = PhNCHS, $\mathrm{CH_2CH_2(C_5H_4N)}$, $\mathrm{CH_2CH_2C(O)OMe}$; M = Mo, W). Photochemical and Chemical Reactions and Isolation of a Trinuclear Complex Having a Coordinatively Unsaturated Ruthenium Atom

Masao Kato,[1a] Masaki Kawano,[1a] Hirokazu Taniguchi,[1a] Mikimasa Funaki,[1a] Hiroshi Moriyama,[1b]
Toshio Sato,[1c] and Kazuko Matsumoto*,[1a]

Received January 3, 1991

Syntheses, structures, and reactivities of the title compounds are reported. $\mathrm{[(PhNCHS)Ru(CO)(PPh_3)]_2(\mu\text{-}MS_4)\cdot 2(CH_3)_2CO}$ (M = Mo (**1**) and M = W (**3**)) undergoes photochemical reaction in the presence of pyridine (py) to afford $\mathrm{[(PhNCHS)Ru(py)_2]_2(\mu\text{-}MS_4)}$ and $\mathrm{[(PhNCHS)Ru(py)_2](\mu\text{-}MS_4)[(PPh_3)(CO)Ru(PhNCHS)]}$. In the reaction with $\mathrm{Me_3NO}$, **1** and **3** give $\mathrm{[(PhNCHS)Ru(PPh_3)](\mu\text{-}MS_4)[(PPh_3)(CO)Ru(PhNCHS)]}$, which has a novel five-coordinated Ru atom. This reaction product further undergoes chemical reaction in the presence of py to give $\mathrm{[(PhNCHS)Ru(py)_2]_2(\mu\text{-}MS_4)}$. Compound **1** crystallizes in the orthorhombic space group *Pbcn* with $a = 30.692$ (4) Å, $b = 8.735$ (2) Å, $c = 22.302$ (4) Å, $V = 5980$ (2) Å^3, and $Z = 4$. Anisotropic refinement of all non-hydrogen atoms converged to the residuals $R = 0.065$ and $R_w = 0.072$ ($w = 1/\sigma^2(F)$). Compound **3** crystallizes in the same space group as **1** with $a = 30.826$ (7) Å, $b = 8.735$ (3) Å, $c = 22.306$ (4) Å, $V = 6000$ (3) Å^3, and $Z = 4$. The final R values were $R = 0.080$ and $R_w = 0.090$ ($w = 1/\sigma^2(F)$).

Introduction

We have attempted to synthesize sulfur-bridged cluster complexes that are robust against ligand substitution, leading to the reactions of coordinated small ligand molecules like nitrogen-fixing enzymes.[2-6] The scope of our research is not limited to the metals relevant to the enzymes but is expanded generally to other metals for constructing cluster frameworks that can endure a wide variety of substitution and redox reactions. In this respect, ruthenium seems advantageous because of its strong π-back-donating ability. In the present study two ruthenium atoms are bridged by $\mathrm{MS_4^{2-}}$ (M = Mo, W) to form trinuclear cluster complexes. Although $\mathrm{MS_4^{2-}}$ compounds have widely been studied as ligands for many transition metals in possible relevance to the biological molecules and a number of binuclear or trinuclear complexes of the type $\mathrm{L_2M'(MS_4)}$,[7] $\mathrm{M'(MS_4)_2}$,[8-10] and $\mathrm{(M'L_n)_2(\mu\text{-}MS_4)}$[11,12] (M′ is the transition element) have been reported, research has still been limited for the employment of $\mathrm{MS_4^{2-}}$ as ligands to simple coordination compounds and only a few compounds are reported where $\mathrm{MS_4^{2-}}$ is coordinated to organometallic groups. We have been interested in the reactivities of organoruthenium cluster complexes involving $\mathrm{MS_4^{2-}}$ and report here the first realization of photochemical or chemical dissociation of a coordinated carbonyl group to produce a five-coordinated ruthenium atom. $\mathrm{MS_4^{2-}}$-bridged trimetallic complexes with a $\mathrm{Ru(\mu\text{-}MS_4)Ru}$ framework and basic ligand substitution reactions have already been reported for other $\mathrm{Ru(\mu\text{-}MS_4)Ru}$ compounds.[13-15] However, the present report is the first example of photochemical substitution in Ru and any other $\mathrm{(M'L_n)_2(\mu\text{-}MS_4)}$ complexes.

Experimental Section

Preparation of the Complexes. All compounds described herein are air-stable, except those containing a five-coordinated Ru atom. The latter

---

(1) (a) Waseda University. (b) Toho University. (c) Tohoku University.
(2) Holm, R. H. *Chem. Soc. Rev.* **1981**, *10*, 455.
(3) Coucouvanis, D. *Acc. Chem. Res.* **1981**, *14*, 201.
(4) Zumft, W. G. *Eur. J. Biochem.* **1978**, *91*, 345.
(5) Palermo, R. E.; Singh, R.; Bashkin, J. K.; Holm, R. H. *J. Am. Chem. Soc.* **1984**, *106*, 2600.
(6) Holm, R. H.; Simhon, E. D. In *Molybdenum Enzymes*: Spiro, T. G., Ed.; Wiley Interscience: New York, 1985; Chapter 1.
(7) Siedel, A. R.; Hubbard, C. R.; Mighell, A. D.; Doherty, R. M.; Stewart, J. M. *Inorg. Chim. Acta* **1980**, *38*, 197.
(8) Bowmarker, G. A.; Boyd, P. D. W.; Sorrenson, R. J.; Reed, C. A.; McDonald, J. W. *Inorg. Chem.* **1985**, *24*, 3.
(9) (a) $\mathrm{M'(MS_4)_2^{2-}}$ (M′ = Ni, Pd, Pt): Callahan, K. P.; Piliero, P. A. *Inorg. Chem.* **1980**, *19*, 2619. (b) $\mathrm{Fe(WS_4)_2^{2-}}$: Stremple, P.; Baenziger, N. C.; Coucouvanis, D. *J. Am. Chem. Soc.* **1981**, *103*, 4601. (c) $\mathrm{Co(WS_4)_2^{2-/3-}}$: Muller, A.; Hellmann, W.; Schimanski, U.; Jostes, R.; Newton, W. E. *Z. Naturforsch., B: Anorg. Chem., Org. Chem.* **1983**, *38*, 528. Muller, A.; Jostes, R.; Flemming, V.; Potthast, R. *Inorg. Chim. Acta* **1980**, *44*, L33.
(10) (a) $\mathrm{Mo_2S_6^{2-}}$, $\mathrm{Mo_2S_7^{2-}}$, and $\mathrm{Mo_2S_9^{2-}}$: Coucouvanis, D.; Hadjikyriacou, A. *Inorg. Chem.* **1987**, *26*, 1. (b) $\mathrm{W_4S_{12}^{2-}}$: Secheresse, F.; LeFebvre, J.; Daran, J. C.; Jeannin, Y. *Inorg. Chem.* **1982**, *21*, 1311. (c) $\mathrm{W_3S_9^{2-}}$: Cohen, S. A.; Stiefel, E. I. *Inorg. Chem.* **1985**, *24*, 4657. (d) $\mathrm{W_3S_8^{2-}}$: Bhaduri, S.; Ibers, J. A. *Inorg. Chem.* **1986**, *25*, 3.
(11) Do, Y.; Simhon, E. D.; Holm, R. H. *Inorg. Chem.* **1985**, *24*, 4635.
(12) (a) $\mathrm{(FeCl_2)_2WS_4^{2-}}$: Coucouvanis, D.; Simhon, E. D.; Stremple, P.; Ryan, M.; Swenson, D.; Baenziger, N. C.; Simopoulos, A.; Papaefthymiou, V.; Kostikas, A.; Petrouleas, V. *Inorg. Chem.* **1984**, *23*, 741. (b) $\mathrm{Au_2(PPh_3)_nMoS_4}$ ($n = 2, 3$): Charnock, J. M.; Bristow, S.; Nicholson, J. R.; Garner, C. D.; Clegg, W. *J. Chem. Soc., Dalton Trans.* **1987**, *303*. (c) $\mathrm{Au_2(PEt_3)_2MoS_4}$: Kinsch, E. M.; Stephan, D. W. *Inorg. Chim. Acta* **1985**, *96*, L87. (d) Manoli, J. M.; Potvin, C.; Secheresse, F.; Marzak, S. *J. Chem. Soc., Chem. Commun.* **1986**, 1557.
(13) Howard, K. E.; Rauchfuss, T. B.; Wilson, S. R. *Inorg. Chem.* **1988**, *27*, 1710.
(14) Greaney, M. A.; Coyle, C. L.; Harmer, M. A.; Jordan, A.; Stiefel, E. I. *Inorg. Chem.* **1989**, *28*, 912.
(15) Tanaka, K.; Morimoto, M.; Tanaka, T. *Inorg. Chim. Acta* **1981**, L61.

0020-1669/92/1331-0026$03.00/0